INTENSITY AND POLARIZATION CHARACTERISTICS ALONG THE EARTH'S SURFACE FOR THE ELF-VLF WAVES EMITTED FROM A TRANSMISSION CONE IN THE HIGH LATITUDE

Isamu NAGANO[1], Masayoshi MAMBO[1], Tetsuya SHIMBO[1]
and Iwane KIMURA[2]

[1]*Department of Electrical Engineering, Kanazawa University, 40-20, Kodatsuno 2-chome, Kanazawa 920*
[2]*Department of Electrical Engineering, Kyoto University, Yoshida Honmachi, Sakyo-ku, Kyoto 606*

Abstract: A computer code has been developed, which incorporates a full-wave treatment of down-going ELF-VLF wave injected at any altitude in the ionosphere. Ground conductivity is included as a variable in the code. The code expands a spatially confined electromagnetic wave into a finite set of plane waves. For each elemental plane wave, the field components are calculated by a full-wave method, and the field distribution is obtained by FFT analysis of the full-wave solutions. In this paper, numerical calculations are carried out for both daytime and nighttime ionosphere models in high latitude. The distributions of intensity as well as polarization on the ground are presented in the case that ELF-VLF waves having a spatial amplitude distribution are injected onto the ionosphere.

1. Introduction

Recently, multi-station simultaneous observations at geomagnetically conjugate points of ELF-VLF natural waves and artificially transmitted VLF waves such as the Siple Station transmission have been carried out on the ground to clarify the generation mechanism of emissions associated with these waves due to the wave-particle interactions (TSURUDA *et al.*, 1982; SATO and KOKUBUN, 1981). According to the experimental results, MACHIDA and TSURUDA (1984) showed that the spatial attenuation rate was ~6 dB/100 km in the vicinity of the wave exit region from where the wave emerges into free space (MACHIDA and TSURUDA, 1984). They also pointed out that this value was appreciably higher than that expected from the previous theoretical work (WALKER, 1974). In order to theoretically support these experimental results, it is necessary to develop a full-wave technique that makes it possible to treat a spatially confined wave packet instead of a plane wave.

We have already developed a numerical technique to deal with one-dimensional Gaussian beam wave and have reported the propagation characteristics of VLF waves propagating through the earth-ionospheric wave guide (NAGANO *et al.*, 1982).

In this paper, the previous technique is extended to make clear the azimuthal dependency of the wave field. We will briefly describe the basic technique of the code, and present the field intensity on the earth surface for the ELF-VLF waves injected with a constant amplitude within the transmission cone at the top of the model

ionosphere. In this calculation, we employed the daytime and nighttime ionospheric models made from actual observation in the auroral zone by the sounding rocket (LERFALE and LITTLE, 1970) since the present calculation is to be compared with the results of analyses of the ELF-VLF waves observed at the multi-stations in Iceland.

2. Basic Theory and Calculation Technique

A Cartesian coordinate system (x,y,z) is used as shown in Fig. 1. We consider a two-dimensional beam wave which has a spatially confined amplitude distribution

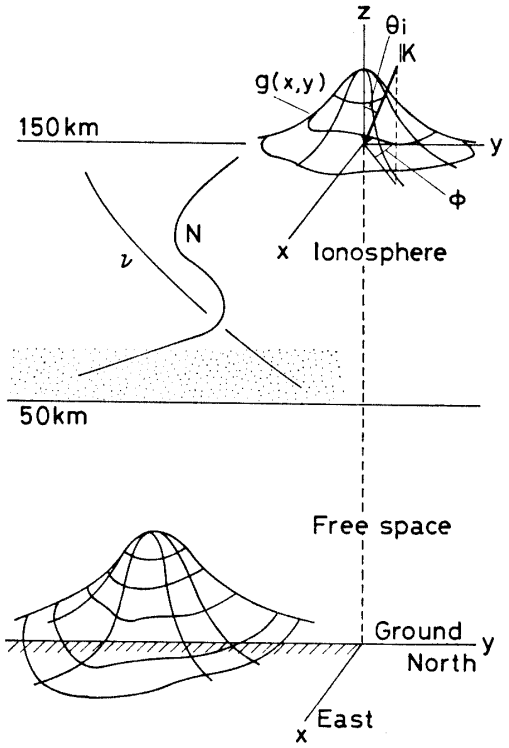

Fig. 1. The schematic structure of the problem.

in the x-y plane. The electromagnetic field of the beam wave $\boldsymbol{E}(x,y,z)$ is expressed as follows:

$$\boldsymbol{E}(x,y,z)=(2\pi)^{-2}\iint_{-\infty}^{\infty}\tilde{\boldsymbol{E}}(k_x,k_y,z)\exp(-j(k_x x+k_y y))\mathrm{d}k_x\mathrm{d}k_y, \tag{1}$$

where $\sim$ denotes the spatial Fourier component, k_x and k_y are the x and y components of the wave vector, respectively. Since the electric field at an arbitary altitude z in the integral of eq. (1), $\tilde{\boldsymbol{E}}(k_x,k_y,z)$, is a plane wave with k_x and k_y, it satisfies the wave equation in the horizontally stratified medium in the coordinates shown in Fig. 1. By using the multi-layered method including the earth effect (NAGANO *et al.*, 1975), we can get the full-wave solution $\tilde{\boldsymbol{F}}(k_x,k_y,z)$ for the elementary plane wave with a unit amplitude. The electric field distribution on the x-y plane at an altitude z can be expressed by

$$\boldsymbol{E}(x,y,z)=(2\pi)^{-2}\iint_{-\infty}^{\infty} C(k_x,k_y)\tilde{\boldsymbol{F}}(k_x,k_y,z)\exp(-j(k_x x+k_y y))\mathrm{d}k_x\mathrm{d}k_y, \tag{2}$$

where $C(k_x,k_y)$ is a weight function determined by the amplitude distribution of the beam wave as follows. We express the spatial distribution of a down-going wave at the incident altitude $z=z_0$ as the function of x and y, $g(x,y)$, which is expanded into a set of plane waves by Fourier integral,

$$g(x,y)=(2\pi)^{-2}\iint_{-\infty}^{\infty} \tilde{G}(k_x,k_y)\exp(-j(k_x x+k_y y))\mathrm{d}k_x\mathrm{d}k_y, \tag{3}$$

$$\tilde{G}(k_x,k_y)=\iint_{-\infty}^{\infty} g(x,y)\exp(j(k_x x+k_y y))\mathrm{d}x\mathrm{d}y, \tag{4}$$

where $\tilde{G}(k_x,k_y)$ is the Fourier component with k_x and k_y. Then, we assume that $g(x,y)$ is equal to the amplitude distribution of $-E_y$ of the down-going right-handed circular polarized whistler mode waves at the incident altitude z_0. $C(k_x,k_y)$ is then equal to $\tilde{G}(k_x,k_y)$. Substituting this into eq. (2) and integrating the full-wave solutions we get the exact solution of the beam wave at other altitudes, as:

$$\begin{aligned}\boldsymbol{E}(x,y,z)=(2\pi)^{-2}\iint_{-\infty}^{\infty} &\tilde{G}(k_x,k_y)\tilde{\boldsymbol{F}}(k_x,k_y,z)/\tilde{E}_y{}^{R\text{-}DOWN}(k_x,k_y,z=z_0)\\ &\exp(-j(k_x x+k_y y))\mathrm{d}k_x\mathrm{d}k_y,\end{aligned} \tag{5}$$

where z_0 denotes the incident altitude. In the numerical calculation, we modify the Fourier integration of eq. (5) to the two-dimensional discrete Fourier transformation as follows: Let us put

$$k_x=\frac{2\pi}{\lambda_0}S_x \quad \text{and} \quad k_y=\frac{2\pi}{\lambda_0}S_y, \tag{6}$$

where λ_0 is the wave length in free space. Further let us write S_x and S_y as

$$S_x=\Delta S_x n \quad \text{and} \quad S_y=\Delta S_y m, \tag{7}$$

where ΔS_x and ΔS_y are small values with the dimensions of S_x and S_y. n and m are dimensionless integers taken as new variables of integrations. Then, eq. (5) can be approximated by the following summation.

$$\begin{aligned}\boldsymbol{E}(\Delta x l,\Delta y h,z)=&\sum_{n=-N/2}^{N/2-1}\sum_{m=-M/2}^{M/2-1}\tilde{D}(\Delta S_x n,\Delta S_y m,z)\\ &\exp\left(-j\left(\frac{2\pi}{\lambda_0}(\Delta S_x\Delta x n l+\Delta S_y\Delta y m h)\right)\right)\Delta S_x\Delta S_y/\lambda_0{}^2,\end{aligned} \tag{8}$$

where $\tilde{D}=\tilde{G}\tilde{F}/\tilde{E}_y{}^{R\text{-}DOWN}$.

In deriving eq. (8), we put $x=\Delta x l$ and $y=\Delta y h$ in a similar manner to eq. (7). On the other hand, Discrete Fourier Transform (DFT) algorithm is expressed by

$$\mathscr{F}_{lh}[x_{nm}]=\sum_{n=0}^{N-1}\sum_{m=0}^{M-1} x_{nm}\exp\left(-j2\pi\frac{nl}{N}\right)\exp\left(-j2\pi\frac{mh}{M}\right), \tag{9}$$

where $l=0,1,\ldots\ldots,N-1$, $h=0,1,\ldots\ldots,M-1$

Comparing eq. (8) with eq. (9), we obtain the conditions

$$\Delta S_x \Delta x=\frac{\lambda_0}{N} \quad \text{and} \quad \Delta S_y \Delta y=\frac{\lambda_0}{M}. \tag{10}$$

Then let us put ΔS_x and ΔS_y as

$$\Delta S_x=\frac{1}{N1} \quad \text{and} \quad \Delta S_y=\frac{1}{M1}, \tag{11}$$

where $N1$ and $M1$ are integers. Eq. (10) put the limitations in the spatial resolutions and in the size of space to be taken into calculation, which are the results of using the DFT algorithm instead of Fourier integral to calculate the beam wave. One of the limitations is for the spatial resolution

$$\Delta x=\frac{N1}{N}\lambda_0 \quad \text{and} \quad \Delta y=\frac{M1}{M}\lambda_0. \tag{12}$$

The other is the limitation of space in the x-y coordinate

$$X=N1\lambda_0 \quad \text{and} \quad Y=M1\lambda_0. \tag{13}$$

In this way we can obtain the two-dimensional amplitude distribution of the beam wave at any altitude. The procedures for the numerical calculation are as follows:

(1) The spectrum function $\tilde{G}(k_x,k_y)$ transformed from the spatial amplitude distribution of the down-going wave, $g(x,y)$, is assumed at the altitude of incidence. We have chosen $\tilde{G}(k_x,k_y)$ as a uniform distribution within the transmission cone.

(2) Eq. (5) is approximated by summing up a finite number of (k_x,k_y), up to a few thousand points, instead of integrating an infinite number of (k_x,k_y) by using the DFT algorithm as expressed in eq. (9). We used the two-dimensional FFT with $2^9\times 2^9$ data points. The values of $N1$ and $M1$ are the same and equal to 2^5. In this case, the spatial resolution on the ground is $\lambda_0/16$. For each elemental wave with k_x and k_y, we can use a full-wave solution taking account of the ground reflection effect obtained by the multi-layered method.

3. Model for Calculation

3.1. A model for the incident wave

As a down-going incident beam wave at the incident altitude, we can select either an arbitrary spatial distribution of field intensity $g(x,y)$ with a specific direction of k vector or a wave expressed by an arbitrary spectrum function $\tilde{G}(k_x,k_y)$. Taking into account the fact that the wave can penetrate the ionosphere to the free space when the k vector lies within the transmission cone, the latter model is adopted in this paper. Namely the following functions are assumed for one- and two-dimensional cases.

For one-dimensional case,

$$\tilde{G}(k_x)=\begin{cases} \dfrac{\lambda_0}{2} & (k_x<2k_0) \\ 0 & (k_x\geqq 2k_0), \end{cases} \tag{14}$$

and, for two-dimensional case,

$$\tilde{G}(k_x,k_y)=\begin{cases} \dfrac{{\lambda_0}^2}{\pi} & ({k_x}^2+{k_y}^2<(2k_0)^2) \\ 0 & ({k_x}^2+{k_y}^2\geqq(2k_0)^2), \end{cases} \tag{15}$$

where k_0 is the wave number in free space. The above functions imply that input k spectra are distributed over the vertical cone whose cone angle is twice the transmission cone angle. The rectangular k spectra assumed here cause an oscillatory field distribution on the ground. This oscillation is due to sharp cutoff of k spectra and not a real one. To reduce this oscillation, k spectra outside transmission cone are necessarily depending on the frequency and ionospheric parameters.

3.2. *Ionospheric and earth's model*

The ionospheric model used in the numerical calculations is shown in Fig. 2.

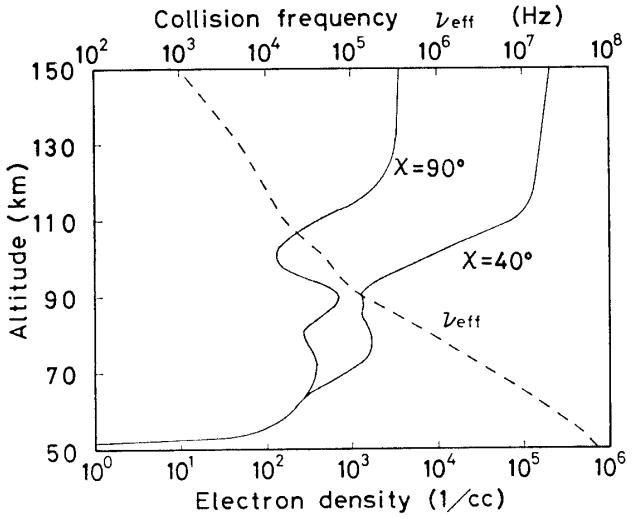

Fig. 2. The electron density and the collision frequency profiles used in the numerical calculation.

Table 1. Parameters used in the numerical calculations.

Incident altitude		150 km
Geomagnetic dip angle	dip	75°
Electron gyrofrequency	f_H	1.54 MHz
The conductivity and dielectric constant of earth		10^{-3} (S/m) and 10
One dimensional case		
Wave frequency	f	0.5, 0.75, 1.0, 1.25, 1.5, 2.0, 3.0, 5.0 (kHz)
Azimuth angle		0° (North-South propagation)
Two dimensional case		
Wave frequency	f	1.5 kHz

We have used two kinds of electron density profiles which were observed in the northern auroral zone during a magnetic quiet time by sounding rockets (LERFALE and LITTLE, 1970). An effective collision frequency profile used for our calculation is also shown in the figure. The other parameters used in this calculation are shown in Table 1. The topside boundary of the ionosphere is assumed to be located at an altitude of 150 km, and the free space is assumed below an altitude of 50 km. The ground is assumed to be a homogeneous medium.

4. Calculated Results for One-Dimensional Case

In order to interpret the results of analysis of the ELF wave data such as ELF hiss, chorus and QP emissions observed at multi-stations in high latitudes (SATO and KOKUBUN, 1980, 1981) were used. In this section, we calculate field intensity and polarization characteristics on the ground for the one-dimensional case.

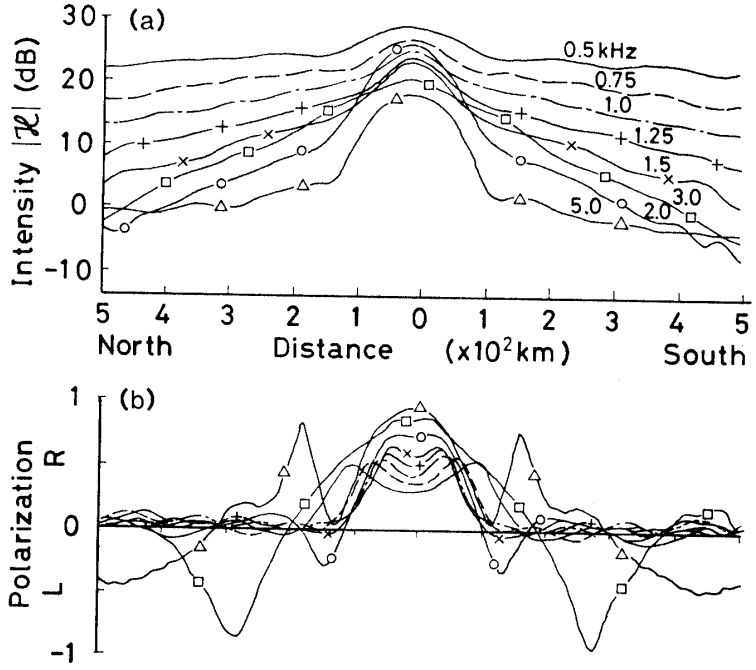

Fig. 3. (a) The field intensities $|\mathcal{H}| = \sqrt{|\mathcal{H}_x|^2 + |\mathcal{H}_y|^2}$ *on the ground as a function of distance from the exit point for the ionospheric model with* $\chi = 40°$ *where* χ *is zenith angle. Numbers by the curves indicate the frequencies used in this calculation. The vertical axis denotes the absolute intensity of the magnetic field when the z component of the Poynting flux of the incident whistler mode wave is 1 W/m². 0 dB is 1 V/m.*
(b) Variation of the polarization vs. distance from the exit point.

4.1. *Frequency dependences of the field intensity and polarization*

Figures 3a and 3b show the field intensities and polarizations along the earth's surface for eight different frequencies in the daytime ionospheric condition. The center of the horizontal axis is the position of the incident wave at an altitude of 150 km. The vertical axis denotes the absolute magnitude of the magnetic field of the wave when the z component of the Poynting flux of the incident whistler mode wave

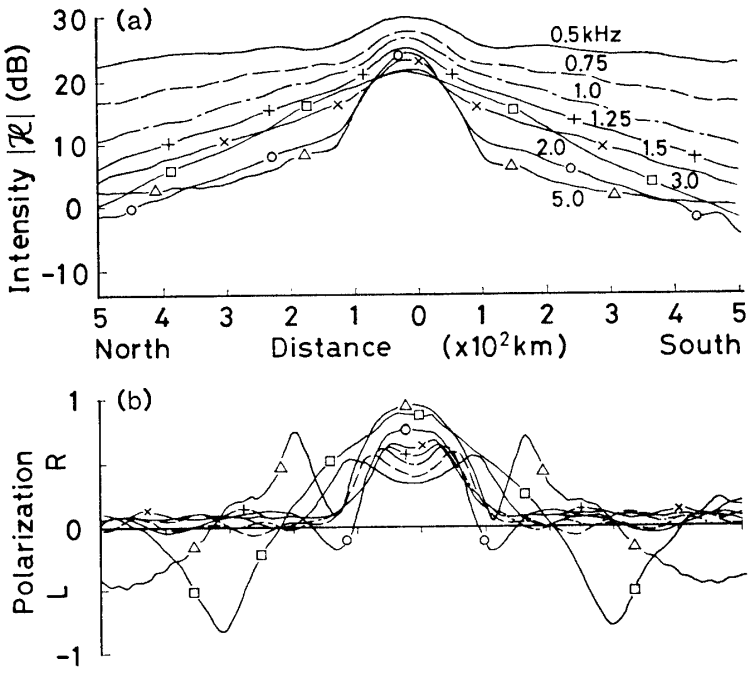

Figs. 4 a, b. Field intensity and polarization vs. distance on the ground from the exit point for the ionospheric model with $\chi=90°$ (refer to Figs. 3a and 3b).

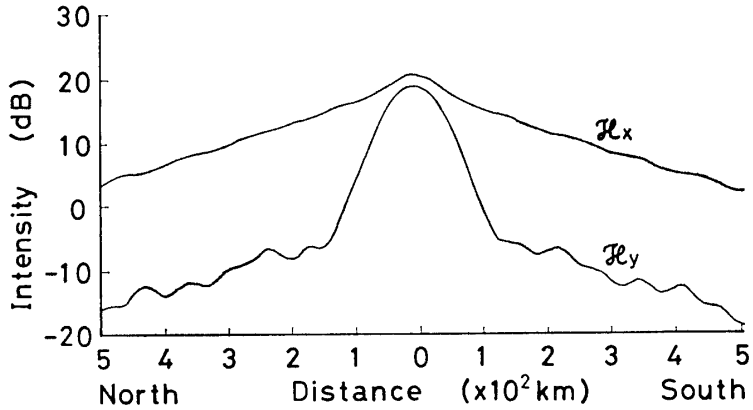

Fig. 5. The field intensities of north-south ($\mathcal{H}_y$) and east-west ($\mathcal{H}_x$) directional components on the ground vs. distance from the exit point for the ionospheric model with $\chi=90°$ at a frequency of 1.5 kHz (refer to Fig. 4).

is 1 W/m². The magnetic intensity which was composed of the north-south and east-west components is illustrated as a field variable with the dimension of electric field, where 0 dB is 1 V/m. The R and L in Fig. 3b indicate the right- and left-handed polarization, respectively. The value of unity denotes a circular polarization.

As is seen in Fig. 3a the attenuation in horizontal direction is extremely large in the distance less than 150 km from the sub-source (or exit) point and it depends slightly on frequency. The wave intensity decreases slowly in the distances far from the exit point.

It is interesting to note that the peak intensity at 2 kHz in the vicinity of (0 km) the exit point is greater than that at 1.5 kHz. This result cannot be simply explained

by the ionospheric absorption because it is greater at 2 kHz than at 1.5 kHz. As will be explained in the latter section, this seems to be due to a resonance effect of the wave propagating between the lower ionosphere and the ground. On the other hand, the polarization of the wave on the ground is almost right-handed circularly polarized in the vicinity of the exit point, but left-handed polarized components appear at great distances. Similarly, Figs. 4a and 4b show the field intensities and polarizations respectively at the sunset or sunrise time (the $\chi=90°$ ionospheric model was used). The attenuation rate with respect to distance shows the same tendency as that in Fig. 3a. But the absolute value of the field intensities in Fig. 4a are slightly large.

Figure 5 shows the field intensities of the north-south ($\mathcal{H}_y$) and east-west ($\mathcal{H}_x$) components as a function of distance at f=1.5 kHz for the ionospheric model of $\chi=90°$. This figure indicates that the field intensity of TE mode attenuates steeply with distance in the vicinity of the exit point.

4.2. The height distribution of the field near the resonance frequency

In order to confirm the resonance effect between the bottom of the ionosphere and the ground surface for waves injected from above, a more simplified assumption for the incident wave is made in this section. Namely a plane wave is assumed to be incident vertically downward onto the ionosphere at an altitude of 150 km.

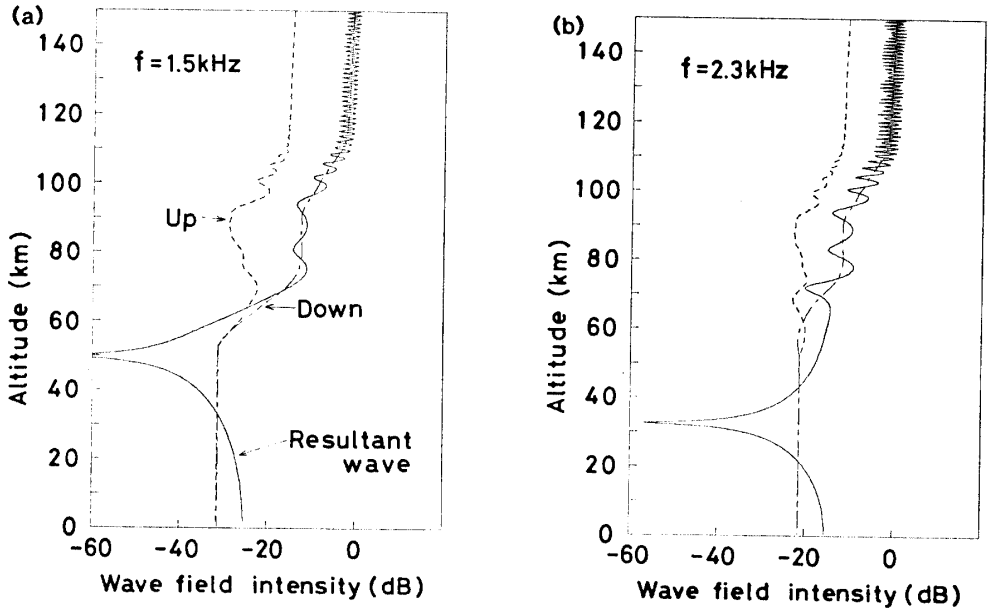

Fig. 6. The height distribution of the horizontal magnetic component at vertically downward incidence for the ionospheric model with $\chi=40°$. The dashed, dot-dashed and solid lines indicate up-going, down-going and resultant waves, respectively. (a) f=1.5 kHz; (b) f=2.3 kHz.

Figures 6a and 6b represent the height distributions of the upgoing, down-going and resultant field intensities of the horizontal magnetic field component normalized by the magnetic field intensity at the incident altitude. The resultant wave field intensity at 2.3 kHz on the ground ($z=0$ km) is about 7 dB higher than that of 1.5 kHz. As can be seen in Fig. 6b, the height at the minimum intensity of the resultant wave is 32.6 km above the ground and it agrees with a quarter of wave length in free space. Therefore, the maximum intensity at 2.0 kHz in the frequency range of 1 kHz to 3 kHz

of Fig. 4a can be explained by this resonance effect. The value of Q was about 4.5. Naturally, the resonance frequency depends on the ionospheric model.

Recently STUBBE *et al.* (1982) reported that signal strength as a function of modulation frequency showed pronounced maxima at multiples of approximately 2 kHz in the experiment on the ionospheric current modulation using powerful amplitude modulated HF waves. Our numerical result on the resonant effect is consistent with their interpretation of the maximum strength at 2 kHz in spite of different ionospheric model.

5. Calculation Results for Two-Dimensional Case

Since it takes a lot of computer time to calculate the wave field for the two-dimensional case, we made the calculation of amplitude distribution of the wave and its polarization patterns on the horizontal plane only for the ionospheric model with $\chi=90°$ and at the frequency of 1.5 kHz which is shown in Figs. 7a and 7b, respectively.

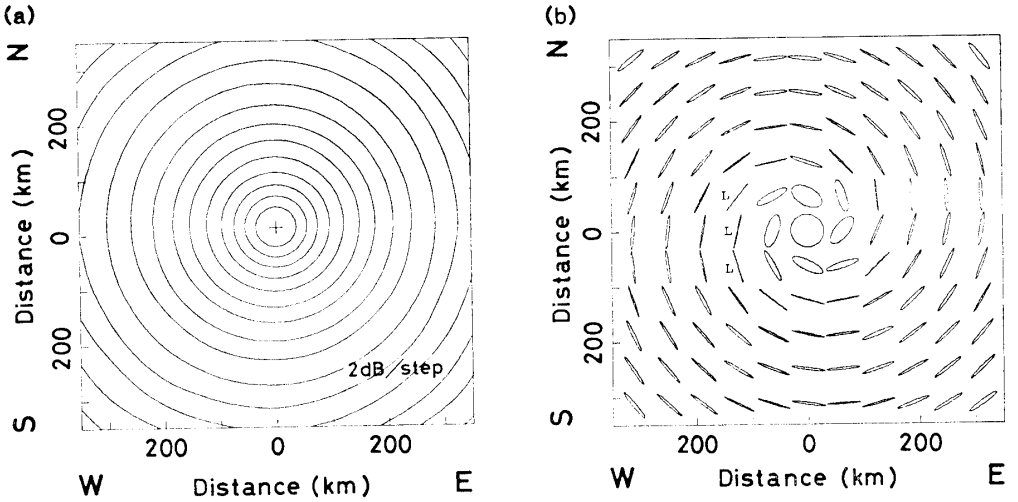

Fig. 7. (a) The contour magnetic field $|\mathcal{H}|$ distribution when the angular spectra of down-going whistler mode wave, incident on the ionosphere, is uniformly spread over the two-dimensional transmission cone. The calculation is carried out at $f=1.5$ kHz for the ionospheric model with $\chi=90°$. The absolute intensity at the center (+) of this figure is 24.8 dB, where 0 dB is taken as 1 V/m when the Poynting flux of the down going whistler wave at the incident altitude is 1 W/m², and the contour lines are plotted every 2 dB attenuation from the center. (b) Polarization patterns at every mesh point of the grid with the unit length of 60 km. The letter L by the pattern indicates the left-handed polarization and the other is the right-handed polarization.

The intensities of the contour lines in Fig. 7a are drawn every 2 dB. The center of the figure indicates the point on the ground where the peak value of the incident wave is observed. The contours with the same amplitude seem to be almost disk-shaped in this result, but it the shape becomes different in the case of higher frequency (NAGANO *et al.*, 1985). The peak value of the field intensity is about 24.8 dB at the center of the figure and it is the same as that of the results in the one-dimensional case (see Fig. 4a). But the attenuation rate as a function of distance on the ground is slightly large as compared with the one-dimensional case. It is very interesting that

the attenuation of the wave field is roughly proportional to 1/R where R is a distance from the point of maximum amplitude. This seems to be due to the small source size.

On the other hand, polarization pattern is plotted at every mesh point of the grid with the unit length of 60 km. The magnitude of major axis in every elliptical polarization is taken as the same. At the distance greater than about 100 km from the center, the wave has almost linear polarization and the direction of it is almost perpendicular to the azimuthal direction. This may suggest that we can predict with high accuracy the direction of the wave coming from the source from the knowledge of the polarization at the long distance from the source point. As for the sense of polarization, the right-handed circular polarization appears in the vicinity of the exit point and it changes to the elliptical polarization still in the right-handed sense but close to the linear polarization outside the 100 km circle from the source.

6. Conclusions

A computer code has been developed, which incorporates a full-wave treatment of down-going VLF wave injected at any altitude in the ionosphere. A model is constructed for a whistler mode wave with wave normal spreading over the transmission cone. Using this calculation technique, we have obtained both field intensity and polarization characteristics of the ELF-VLF waves in the frequency range from 0.75 to 5 kHz for the actual ionospheric models observed by the rocket in auroral zone.

The major points we have discussed in this paper are as follows:

(1) The attenuation rate is about 8–9 dB/100 km in the vicinity of the exit point from which the wave emerges into the free space and it is about 2 dB/100 km at long distance from the exit point.

(2) There is a resonance effect caused by the wave of the frequency of 2.3 kHz propagating between the earth's surface and the lower ionosphere.

(3) According to the two-dimensional results, we may be able to predict with high accuracy the direction of wave normal coming from the exit point at long distance from the source.

Acknowledgments

The authors wish to express their thanks to Dr. N. SATO and Mr. H. YAMAGISHI for supporting this study. We are also grateful to Mr. S. MORITA of Kanazawa University for tracing the figures in this paper.

References

LERFALE, C. M. and LITTLE, C. G. (1970): *D*-region electron temperatures at the northern auroral zone. Radio Sci., **12**, 1017–1028.

MACHIDA, S. and TSURUDA, K. (1984): Intensity and polarization characteristics of whistlers detected from multi-station observations. J. Geophys. Res., **89**, 1675–1682.

NAGANO, I., MAMBO, M. and HUTATSUISHI, G. (1975): Numerical calculation of electromagnetic waves in an isotropic multi-layered medium. Radio Sci., **10**, 611–617.

NAGANO, I., MAMBO, M., YOSHIZAWA, S., KIMURA, I. and YAMAGISHI, H. (1982): Full wave calculation for a gaussian VLF wave injection into the ionosphere. Mem. Natl Inst. Polar Res., Spec. Issue, **22**, 46–57.

NAGANO, I., MAMBO, M. and FUKAMI, T. (1985): Wave intensity distribution on the ground for downgoing the gaussian VLF wave injected into ionosphere. Proceeding of Sino-Japanese Joint Meeting on OFSET, 433–436.

SATO, N. and KOKUBUN, S. (1980): Interaction between ELF-VLF emissions and magnetic pulsations; Quasi-periodic ELF-VLF emissions associated with Pc 3–4 magnetic pulsations and their geomagnetic conjugacy. J. Geophys. Res., **85**, 101–113.

SATO, N. and KOKUBUN, S. (1981): Interaction between ELF-VLF emissions and magnetic pulsations; Regular periodic ELF-VLF pulsations and their geomagnetic conjugacy. J. Geophys. Res., **86**, 9–18.

STUBBE, P., KOPKA, H., RIETVELD, M. T. and DOWDEN, R. L. (1982): ELF and VLF wave generation by modulated HF heating of the current carrying lower ionosphere. J. Atmos. Terr. Phys., **44**, 1123–1135.

TSURUDA, K., MACHIDA, S., TERASAWA, T., NISHIDA, A. and MAEZAWA, K. (1982): High spatial attenuation of the Siple transmitter signal and natural VLF chorus observed at ground-based chain stations near Roberval, Quebec. J. Geophys. Res., **87**, 742–750.

WALKER, A. D. M. (1974): Excitation of earth-ionosphere wave guide by down going whistlers. Proc. R. Soc. London, Ser. A, **340**, 367–394.

(Received October 2, 1985; Revised manuscript received December 20, 1985)